

# Sorption of thorium(IV) from aqueous solutions by graphene oxide

Yan Li · Chunli Wang · Zhijun Guo ·  
Chunli Liu · Wangsuo Wu

Received: 23 September 2013 / Published online: 23 January 2014  
© Akadémiai Kiadó, Budapest, Hungary 2014

**Abstract** Graphene oxide (GO) is one of the most important carbon nano-materials. In this paper, GO was synthesized from flake graphite and characterized by transmission electron microscopy, atomic force microscopy, and X-ray photoelectron spectroscopy. The sorption of Th(IV) on GO was investigated as a function of contact time, solid-to-liquid ratio, pH, ionic strength, and in the presence of fulvic acid (FA) and humic acid (HA) by batch experiments. The sorption percentage of Th(IV) on GO decreased with increasing ionic strength and decreasing solid-to-liquid ratio. The sorption edge of Th(IV) in the presence of FA/HA is much lower than that in the absence of FA/HA. Furthermore, the sorption processes of Th(IV) can be described by a pseudo-second order rate model. Based on the Langmuir model, the maximum sorption capacities ( $C_{s_{max}}$ ) of Th(IV) were about  $5.80 \times 10^{-4}$  mol/L. From thermodynamic investigation, sorption of Th(IV) on GO is spontaneous and endothermic in nature. The rapid sorption rate and high sorption capacity suggest that GO is a promising adsorbent for Th(IV).

**Keywords** Sorption · Th(IV) · Graphene oxide · Sorption capacity

Y. Li · C. Wang · C. Liu  
Beijing National Laboratory for Molecular Sciences,  
Fundamental Science Laboratory on Radiochemistry &  
Radiation Chemistry, College on Chemistry and Molecular  
Engineering, Peking University, Beijing 100871, People's  
Republic of China  
e-mail: liucl@pku.edu.cn

Z. Guo · W. Wu (✉)  
Radiochemistry Laboratory, School of Nuclear Science and  
Technology, Lanzhou University, Lanzhou 730000, Gansu,  
People's Republic of China  
e-mail: wuws@lzu.edu.cn

## Introduction

Graphene nanosheets (GNS) are newly emerging members of carbon materials with a hexagonal,  $sp^2$ -hybridized, and one-atom-thick layers structure [1, 2]. Graphene oxide (GO) with multiple oxygen containing functional groups, such as hydroxyl and epoxide groups in the basal plane and carboxyl groups at the plane edges [3, 4] can be easily prepared by chemical modification. Based on the literature, the adsorption sites of heavy metal cations on carbonaceous materials can be categorized into three groups: (1) mineral impurities such as ash and metal oxides contained in carbons [5]; (2) acidic oxygen groups, particularly carboxylic and lactonic groups [6–8]; and (3) basic oxygen centers such as chromenes, ketones, and pyrones [9, 10], basic nitrogen centers such as pyridine [10], and basic sites as  $C_p$  electrons on graphene layers [11]. Experimental studies and theoretical calculations have shown that GNS-based materials possess a high adsorption capacity [12–16]. For example, Yang et al. [17] measured the sorption isotherm of  $Cu^{2+}$  on GO, and then speculated that the interaction between  $Cu^{2+}$  and the sorbent mostly occurs on the carboxyl groups of GO. Li et al. [18] studied the sorption of uranium(VI) on GO and graphene, and found that the sorption capacity on GO and graphene were 299 and 47 mg/g, respectively, which suggests that the acidic oxygen-containing functional groups playing an important role in sorption.

As a toxic radioactive element, thorium(IV) is usually regarded as the representative chemical analogue of tetravalent actinides, which are difficult to maintain in a pure form. Thorium can be used as an alternate nuclear fuel by converting it into  $^{233}U$  in thorium-based molten salt reactor nuclear power systems. Furthermore, Th(IV) and its compounds and alloys have a wide range of uses in industry. For example, thorium oxide has applications as a catalyst, a

high temperature ceramic, and in high quality lenses [19]. The presence of thorium results in two types of hazards: (1) ingestion of an  $\alpha$ -ray internal exposure member of thorium and (2) the proximity to  $\gamma$ -ray emitters with strong penetration ability. In view of the extensive use and the hazards [20], the preconcentration/separation of Th(IV) through sorption is important in nuclear/radiation, environmental, and waste treatment chemistry [21]. Sorption is one of the most important factors that affects the migration of Th(IV) in natural environments [22]. The sorption of Th(IV) onto various materials surfaces has been studied with clay minerals [23–28], TiO<sub>2</sub> [29], gibbsite [30], anatase [31], goethite [32], silica [33, 34], alumina [35] and activated carbon [19]. Based on the large surface area of nano-material, Chen et al. [36] studied the sorption of Th(IV) on multi-wall carbon nanotubes and found that adsorption is an endothermic and spontaneous process with a maximum sorption capacity of 57.14  $\mu\text{mol/g}$ . Few work on the sorption of Th(IV) on GO has been reported. In this paper, with the aims to highlight the possible application of GO as a suitable adsorbent for the removal of Th(IV) from aqueous solution, we synthesized few-layered GO nano-sheets using a modified Hummers method; investigated the influence of pH, ionic strength,  $m/V$  ratio, foreign ions and humic acid (HA) on the sorption of Th(IV) onto GO; studied the sorption kinetics of Th(IV) on GO; simulated sorption isotherm data with Freundlich and Langmuir models and calculated the thermodynamic data.

## Experimental

### Materials

Natural flake graphite (325 mesh) was supplied by Alfa Aesar (Tianjin, PR China) (99.8 % metals basis). Thorium stock solutions were prepared from ThO<sub>2</sub> (purity >99 %, A.R. grade). Fulvic acid (FA) was obtained from Gong Xian weathered coal (Henan Province, PR China). The properties of FA were as follows: the elemental composition (%) was C 55.95, H 2.01, N 1.11, S 1.03, and O 39.90, the number average molecular weight was 1,300 Da, and the capacities of carboxyl and phenol groups were 8.16 and 1.76 meq H<sup>+</sup>/g, respectively. HA was extracted from the soil of Lintai country (Gansu, PR China) and the main elements were C 60.44 %, H 3.53 %, N 4.22 %, O 31.31 %, and S 0.50 %. All other chemicals used were of analytical grade.

### Preparation of GO

GO was synthesized from flake graphite by the modified Hummers method [2–4, 37–39]. In brief, 12 mL H<sub>2</sub>SO<sub>4</sub> and 1.56 g KMnO<sub>4</sub> were added dropwise to 300 mg graphite in a

250 mL flask. The suspension was acutely stirred in an ice bath. The addition was carefully controlled to prevent the temperature getting too high. Then, the ice bath was removed and the suspension was stirred for 2 h. After 2 h, 25 mL water was added dropwise to the suspension in an ice bath. The sample was then heated to 98 °C and refluxed for 30 min. The suspension was cooled down to room temperature and 75 mL water was added in dropwise fashion. The sample was treated with 8 mL 36 % H<sub>2</sub>O<sub>2</sub> to reduce the manganese in higher oxidation states to Mn<sup>2+</sup>. The precipitate was washed with 10 % HCl and deionized water was added until there was no SO<sub>4</sub><sup>2-</sup> detected and the solution reached neutral pH. The precipitate was aged for 48 h at 60 °C and then dialyzed with ultra-pure water (18 M $\Omega$ ) for 2 weeks to remove the remaining salt impurities. The precipitates were separated and dried at 40 °C. Finally, the sample was milled through a 160 mesh screen prior to use.

### Sorption procedures

All sorption experiments were carried out at 25  $\pm$  2 °C. A stock suspension of GO ( $m/V = 0.5$  g/L) was prepared in NaCl solution (0.01, 0.1, 0.5 mol/L). The pH of the suspension was adjusted with negligible volumes of 0.1 mol/L (or 0.01 mol/L) HCl or NaOH solutions to achieve the desired pH values. The tubes were then made up to 6 mL with Th(IV) and shaken for 2 days. The suspension was separated by centrifugation at 18,000 $\times g$  for 30 min. The concentration of Th(IV) [32, 40, 41] in the supernatant was analyzed using the arsenazo(III) complex at 664 nm. The concentration of FA or HA in the supernatant was determined at 200 nm on a Perkin Elmer Lambda 35 UV/VIS spectrometer.

The formulas for the calculation of the solid phase concentration ( $q$ , mol/g) and distribution coefficient ( $K_d$ , mL/g) [42, 43] were

$$q = (C_0 - C_{\text{aq}}) \times \frac{V}{m} \quad (1)$$

$$K_d = \frac{(C_0 - C_{\text{aq}})}{C_{\text{aq}}} \times \frac{V}{m} \quad (2)$$

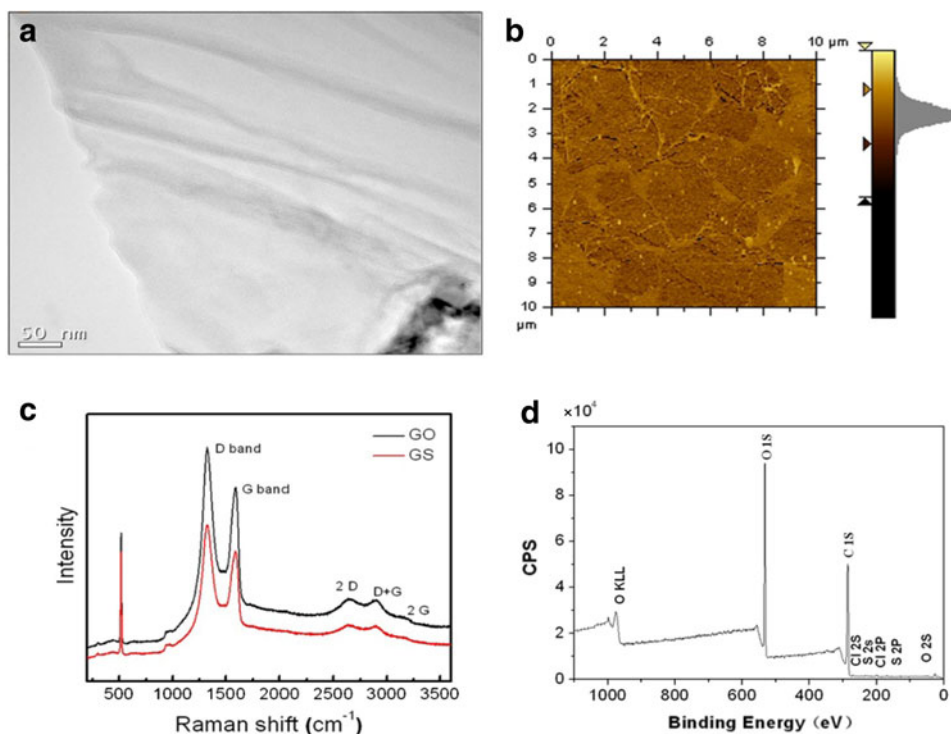
where  $C_0$  is the initial concentration of Th(IV) in the solution,  $C_{\text{aq}}$  is the concentration of Th(IV) in the supernatant after centrifugation (mol/L),  $V$  (L) is the volume of aqueous solution, and  $m$  (g) is the mass of GO.

## Results and discussion

### Characteristics of GO

The obtained samples of GO were characterized by transmission electron spectroscopy (TEM), atomic force microscopy

**Fig. 1** **a** TEM image of GO. **b** AFM image of GO. **c** Raman spectrum of GO. **d**  $C_{1s}$  XPS spectrum of GO



(AFM) and X-ray photoelectron spectroscopy (XPS). The  $pH_{pzc}$  (point of zero charge) value of the GO nanosheets was obtained by mass titration technique [44].

Figure 1a shows the TEM image of GO, which indicates that the thickness of the GO sheets are only several nanometers and the layers are nearly transparent with some crumples [45, 46]. Luo et al. [39] reported that GO are coin-stacked along the (001) fiber growth direction.

Figure 1b shows the AFM image of GO and gives the outline of GO, which indicates that the GO nanosheets have a size of 300 nm to 2  $\mu\text{m}$  with a height of 1 nm. Some folds and small wrinkles can be seen at the edge of the GO in the AFM image. It can be concluded that there is complete exfoliation of GO down to individual GO sheets.

The Raman spectra of GO is shown in Fig. 1c. The typical D band ( $1322\text{ cm}^{-1}$ ) [47] is associated with the vibration of  $sp^3$  carbon atoms of defects and disorder. The G band ( $1595\text{ cm}^{-1}$ ) is connected with the scattering of electrons (by phonons and defects) and  $sp^2$  carbon networks [39, 48, 49].

The  $C_{1s}$  XPS of GO (Fig. 1d) can be divided into four components, which correspond to carbon atoms in different oxygen-containing functional groups. The peak at a binding energy of 284.80 eV can be attributed to the non-oxygenated ring C atoms. It has been reported that the peaks found at shifts of +1.5, +2.5 and +4.0 eV from the main peak can be attributed to the functional groups C–O, C=O, and O=C–O, respectively [50]. The curve fitting results of the C1 XPS are shown in Table 1 as below:

**Table 1** Relative content of functional groups in  $C_{1s}$  spectrum from XPS

	C–C	C–OH/C–O–C	C=O/C–O–C	COOH/COOR
%	45.67	40.23	8.35	5.75

(a) nonoxygenated C at 284.80 eV: 45.67 %; (b) alcohol, ether group at 286.94 eV: 40.23 %; (c) carbonyl at 288.61 eV: 8.35 %; (d) carboxylate at 289.99 eV: 5.75 %. As discussed previously, it is clear that the GO nanosheets are highly oxidized and the main oxygen-containing functional groups are C–O, C=O and O=C–O, which are expected to form strong surface complexes with metal ions [51].

The  $pH_{pzc}$  of GO was determined to be 2.09 from the mass titration technique [44]. The surface area of GO was  $36.56\text{ m}^2/\text{g}$  by BET analysis. The pore size and pore volume calculated from the BET model were 4.70 nm and  $4.30 \times 10^{-2}\text{ cm}^3/\text{g}$ , respectively. The average surface area and pore size of graphene prepared by Deng et al. [46] were  $14.18\text{ m}^2/\text{g}$  and 9.58 nm, respectively, which shows that graphene is a microporous material.

#### Sorption kinetics of Th(IV) sorption

The Th(IV) sorption percentage as a function of contact time is shown in Fig. 2. Figure 2 shows that sorption of Th(IV) on GO rapidly increases at the initial stage and then

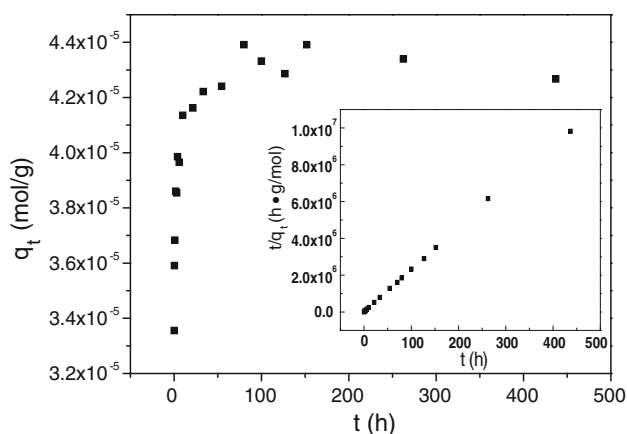


**Fig. 2** Sorption kinetics of Th(IV) on GO.  $I = 0.1$  mol/L NaCl,  $T = 25 \pm 1$  °C,  $m/V = 0.5$  g/L, and pH  $2.80 \pm 0.05$

the sorption remains constant with increasing time. The sorption rapidly achieves equilibrium suggests it is dominated mainly by chemical sorption rather than physical sorption. Generally, metal ion sorption onto materials can be considered as a heterogeneous reaction between the solid and the solution. As point out in several studies [32, 52, 53], sorption can be divided into at least two processes: a very fast process (a chemical reaction with the functional groups), and a slower process (mass transfer through the liquid film surrounding the sorbent and diffusion through the particle pores). Therefore, a time of 24 h was selected to achieve sorption equilibration. The process of adsorption achieved equilibrium in a short time, suggesting that the sorbent has very high adsorption efficiency and potential industrial applications [54].

To analyze the adsorption rate of Th(IV) on GO, a pseudo-second-order rate equation was used to simulate the kinetic adsorption:

$$\frac{t}{q_t} = \frac{1}{k_2 q_e^2} + \frac{1}{q_e} t \quad (3)$$

where  $k_2$  [g/(mol h)] is the pseudo-second-order rate constant of sorption,  $q_t$  (mol/g of dry weight) is the amount of Th(IV) adsorbed on the surface of GO at time  $t$ .  $q_e$  (mol/g of dry weight) is the equilibrium adsorption capacity of Th(IV) on GO. A linear plot of  $t/q_t$  versus  $t$  was achieved and is shown in Fig. 4. The  $k'$  and  $q_e$  values calculated from the slope and intercept were  $2.09 \times 10^4$  g/(mol h) and  $4.41 \times 10^{-5}$  mol/g, respectively. The low value of  $k'$  suggests that the sorption of Th(IV) rapidly achieved equilibrium [23]. The correlation coefficient ( $R^2 = 0.999$ ) indicates that the kinetic adsorption is well described by a pseudo-second-order rate equation.

The sample before and after sorption was characterized by XPS (Table 2). The BEs binding energies of  $O_{1s}$  before and after sorption were 532.79 and 532.63 eV, respectively, which can be explained as a decrease of electron

**Table 2** Variation of surface composition of GO before and after sorption

Sample	Binding energies (eV)			Content (%)		
	$O_{1s}$	Th $4f_{5/2}$	Th $4f_{7/2}$	C	O	Th
GO before sorption	532.79	–	–	67.19	32.81	0
GO after sorption	532.63	334.52	335.1	67.59	31.55	0.86

density around the O atom resulting from electron transfer to Th(IV). On the other hand, the distinct peaks of Th  $4f_{7/2}$  (335.10 nm) and Th  $4f_{5/2}$  (344.52 nm) represent the existence of Th(IV) after sorption. Furthermore, the peak of Th  $4f_{7/2}$  can be attributed to the formation of  $ThO_2$  or  $ThCl_4$  [55], while the peak of Th  $4f_{5/2}$  is related to  $ThO_2$  [56]. Overall, we assume that the sorption of Th(IV) probably occurs on the oxygen functional groups of GO. The process can be written as follows:



where  $\equiv SO^-$  is the negatively charged groups on the surface of GO. As shown in Table 2, the total fraction of Th(IV) was 0.86 %.

#### Effect of pH

pH is an important variable parameter for the sorption of Th(IV) on the porous adsorbent, and it influences the metal speciation in aqueous and solid phases [57]. As shown in Fig. 3, the sorption of Th(IV) on GO increased from 30 to 100 % in the pH range 1.2–3.0, and then remained constant with further increasing pH. It is known that at low pH ( $\leq 2.5$ ) the dominant species of Th(IV) is  $Th^{4+}$  (about 70 %), whereas  $Th(OH)_4$  ( $k_{sp} = 2.0 \times 10^{-45}$ ) is the only species at  $pH \geq 5$ . In this work, the concentration of Th(IV) was  $2.5 \times 10^{-4}$  mol/L, and the precipitate  $Th(OH)_4(s)$  was not formed at  $pH < 3$ . At low pH [58],  $H^+$  can also adsorb onto the surface of GO and occupy the availability active sites of GO. On the other hand, the high positive charge density on the surface of GO at low pH can be another reason for the low sorption capacity. In aqueous solution, the concentrations of surface species ( $\equiv SOH$  uncharged surface groups,  $\equiv SOH_2^+$  positive charged surface groups, and  $\equiv SO^-$  negatively charged groups) change at different pH values. The  $pH_{pzc}$  of GO is determined to be 2.09 from the mass titration technique. The surface species of GO are the negatively charged groups  $\equiv SO^-$  when the pH value is higher than  $pH_{pzc}$  (2.09) and the electrostatic forces between the adsorbent surface and adsorbate ions are then attractive, which is beneficial for the sorption of Th(IV) on GO. With increasing pH, the amount of negatively charged

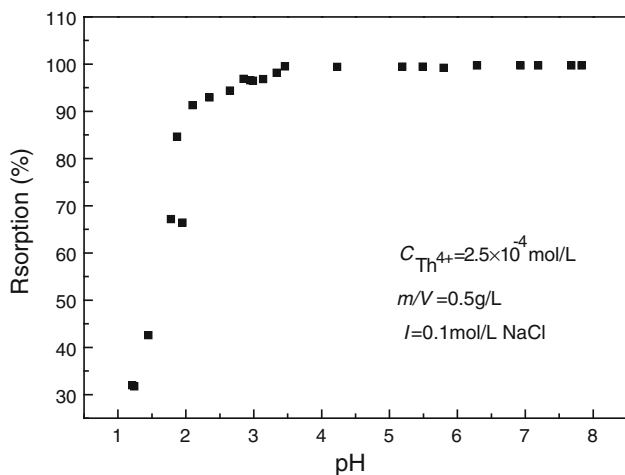


**Fig. 3** Sorption of Th(IV) on GO as a function of pH  $C(\text{Th(IV)}) = 2.44 \times 10^{-4} \text{ mol/L}$ ,  $T = 25 \pm 1 \text{ }^\circ\text{C}$ , and  $m/V = 0.5 \text{ g/L}$

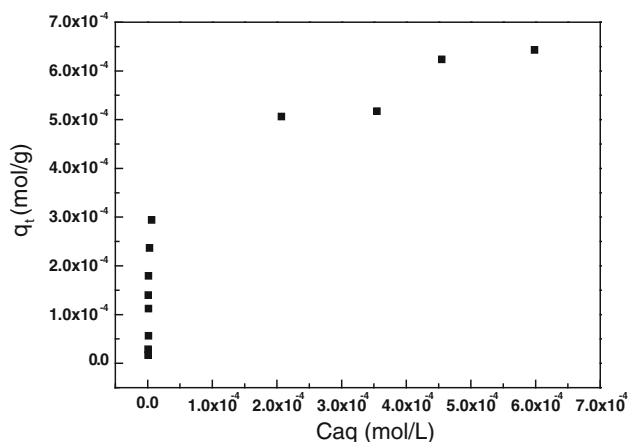


**Fig. 4** Sorption isotherms of Th(IV) on GO.  $T = 25 \pm 1 \text{ }^\circ\text{C}$ ,  $m/V = 0.5 \text{ g/L}$ ,  $\text{pH } 2.80 \pm 0.05$ , and  $I = 0.1 \text{ mol/L}$

$\equiv \text{SO}^-$  groups increases as well as the hydrolysis of Th(IV), which leads to the increase of Th(IV) sorption.

Sorption isotherm

Figure 4 shows the adsorption isotherm of Th(IV) on GO with a pH value of  $2.80 \pm 0.05$ . The experimental data was

analyzed using Langmuir and Freundlich models. The adsorption isotherm is fundamental in describing the interactive behavior between adsorbent and adsorbate. The Langmuir model was developed to represent chemisorption on a set of well-defined localized adsorption sites with the same sorption energy independent of surface coverage and no interaction between adsorbed molecules, whereas the Freundlich model is an empirical model allowing for multilayer adsorption on the adsorbent [22]. The equations of the Langmuir (Eq. 5) and Freundlich (Eq. 6) models are expressed by the following equation:

$$C_s = \frac{q_m k_d C_e}{1 + k_d C_e} \tag{5}$$

$$C_s = k_f C_e^{1/n} \tag{6}$$

where  $C_s$  is the amount of Th(IV) sorbed per mass unit of GO (mol/g),  $q_m$  (mol/g) is the maximum adsorption capacity of Th(IV) per unit weight of adsorbent, and  $k_f$  and  $k_d$  are isotherm constants. The value of  $k_d$  is related to the affinity of the binding sites and is a measure of the energy of adsorption. The separation factor  $R_L$  [53, 59, 60] is a dimensionless constant that is used to predict if adsorption is favorable or unfavorable, and is defined as

$$R_L = \frac{1}{1 + K_d \times C_e} \tag{7}$$

The equations and correlation coefficients ( $R^2$ ) are listed in Table 3. The maximum adsorption capacity of Th(IV) on GO is  $\sim 5.80 \times 10^{-4} \text{ mol/L}$  at  $25 \text{ }^\circ\text{C}$  from the equation of the Langmuir model. The value of  $R_L$  is in the range  $0 < R_L < 1$ , which indicates that adsorption is favorable. As shown in Table 3, the higher correlation coefficients for the Freundlich model indicate that this model fits the sorption data better than the Langmuir model at  $T = 313 \text{ K}$ . From the equation of the Freundlich, the value of  $1/n = 0.3773$  ( $1 < n < 10$ ) indicates that the sorption capacity is only slightly suppressed at lower equilibrium concentration and that sorption is favorable under our experimental conditions. Compared with the other adsorbents listed in Table 4, the performance of GO is also competitive, ranking it among the most effective sorbents for Th(IV) removal. The large sorption capacity of GO for Th(IV) might be because of its high oxidation degree and large specific surface area [18].

**Table 3** Calculated parameters of Freundlich and Langmuir models

$T$ (K)	Langmuir			Freundlich		
	$K_d$ (L/mol)	$q_m$ (mol/g)	$R^2$	$k_f$ (mol $^{n+1}$ / (g $\times$ L $^n$ ))	$1/n$	$R^2$
298.15	$1.75 \times 10^5$	$5.80 \times 10^{-4}$	0.9486	0.0046	0.2647	0.9271
313.15	$1.77 \times 10^5$	$6.90 \times 10^{-4}$	0.9214	0.0065	0.2753	0.9656
338.15	$1.96 \times 10^5$	$7.70 \times 10^{-4}$	0.9194	0.0070	0.2646	0.9641

**Table 4** Maximum sorption capacity of various adsorbents for Th(IV) ions

Adsorbents	$q_m$	Conditions	Ref.
Oxidized multi-wall carbon nanotubes	57.14 $\mu\text{mol/g}$	pH 1.9 $T$ : 293 K	[57]
SiO <sub>2</sub>	1.0 $\mu\text{mol/g}$	pH 3.5 $T$ : 298 K	[35]
SiO <sub>2</sub> + HA	2.05 $\mu\text{mol/g}$	pH 3.5 $T$ : 298 K	[35]
SiO <sub>2</sub> + FA	2.45 $\mu\text{mol/g}$	pH 3.5 $T$ : 298 K	[35]
$\gamma$ -Al <sub>2</sub> O <sub>3</sub>	0.0644 mmol/g	pH 3.5 $T$ : 298 K	[37]
$\gamma$ -Al <sub>2</sub> O <sub>3</sub> + HA	0.176 mmol/g	pH 3.5 $T$ : 298 K	[37]
$\gamma$ -Al <sub>2</sub> O <sub>3</sub> + FA	0.251 mmol/g	pH 3.5 $T$ : 298 K	[37]
Conventional SIR	0.1934 mmol/g	pH 6.0 $T$ : 298 K	[55]
Modified SIR	0.2873 mmol/g	pH 6.0 $T$ : 298 K	[55]
PAN/zeolite	0.04 mmol/g	pH 4.0 $T$ : 298 K	[24]
Zr <sub>2</sub> O(PO <sub>4</sub> ) <sub>2</sub>	6.503 $\mu\text{mol/g}$	pH 2.9 $T$ : 298 K	[54]
MX-80 bentonite	40 mmol/g	pH 1.6 $T$ : 298 K	[26]
Na-bentonite	66 mmol/g	pH 3.5 $T$ : 298 K	[27]
MOR4	1.18 mmol/g	pH 1.0 $T$ : 303 K	[58]
Diatomite	81.51 $\mu\text{mol/g}$	pH 3.0 $T$ : 303 K	[28]
TiO <sub>2</sub>	0.215 mmol/g	pH 3.0 $T$ : 298 K	[33]
TiO <sub>2</sub> + HA	0.229 mmol/g	pH 3.0 $T$ : 298 K	[33]
TiO <sub>2</sub> + FA	0.232 mmol/g	pH 3.0 $T$ : 298 K	[33]
Goethite	6.94 $\mu\text{mol/g}$	pH 2.9 $T$ : 298 K	[34]
Al-pillared rectorite	0.131 mmol/g	pH 1.88 $T$ : 293 K	[59]
Al-MCM-41	92.6 mmol/g	pH 3.4 $T$ : 293 K	[60]
GO	0.58 mmol/g	pH 2.9 $T$ : 298 K	This work

The thermodynamic parameters for the adsorption of Th(IV) on GO were evaluated by the sorption isotherm data obtained at different temperatures. The Gibbs free

energy ( $\Delta G^0$ ), enthalpy ( $\Delta H^0$ ), and entropy ( $\Delta S^0$ ) are related to the Langmuir constant ( $K_d$ ) by

$$\Delta G^0 = -RT \ln K_d \quad (8)$$

$$\Delta S = \frac{\Delta H - \Delta G_1}{T_1} = \frac{\Delta H - \Delta G_2}{T_2} \quad (9)$$

$$\Delta H^0 = R \frac{T_1 T_2}{T_2 - T_1} \ln \frac{K_d(T_2)}{K_d(T_1)} \quad (10)$$

where,  $K_d(T_1)$  and  $K_d(T_2)$  are the Langmuir constants at the temperature  $T_1$  and  $T_2$ , respectively. The negative values of  $\Delta G^0$  (−29.91, −31.45 and −34.24 kJ/mol at 298, 313, and 338 K, respectively) indicates that sorption of Th(IV) on GO is thermodynamically feasible and spontaneous [58, 61] at room temperature. The  $\Delta G^0$  values obtained are between physisorption and chemisorption. The negative value of  $\Delta H^0$  (3.59 kJ/mol) confirms that the adsorption is endothermic in nature. The  $\Delta S^0$  [88.32 J/(mol K)] value may be because of the structural change of GO after sorption.

#### Effect of ionic strength and solid-to-liquid ratio

As shown in Fig. 5, the sorption of Th(IV) decreased when the concentration of the background electrolyte was increased from 0.005 to 0.5 mol/L. Generally, ion exchange and outer-sphere complexes are more affected by ionic strength than inner-sphere complexes [33, 35, 62, 63]. The ions in solution may also influence the double layer thickness and interface potential, and thereby affect the binding of the sorbed species. As the ionic strength increases, the higher concentration of electrolyte ions can generate a thinner double layer, limiting the interaction between the adsorbate and the adsorbent surface and decreasing adsorption [64]. We study the effect of ionic strength at pH  $2.8 \pm 0.05$ , the surface charge of GO is negative. In such a system the electrostatic forces between the adsorbent surface and the adsorbate ions are mainly attractive, an increase in ionic strength will decrease the adsorption capacity. However, in previous work we found that the sorption of Th(IV) on goethite [32], TiO<sub>2</sub> [29], and attapulgite [28] was insensitive to ionic strength. This suggests that the GO has different surface characteristics from those sorbent which lead to various ionic strength dependent.

The influence of the  $m/V$  ratio on the sorption of Th(IV) on GO is shown in Fig. 6. The results indicate that the  $m/V$  ratio plays an important role in the sorption process of Th(IV) on GO. It was found that the higher the solid-to-liquid ratio, the lower the equilibrium Th(IV) concentration in the aqueous phase. Yan et al. [32], Wu et al. [28], and Qian et al. [65] found that the sorption percent of Th(IV)

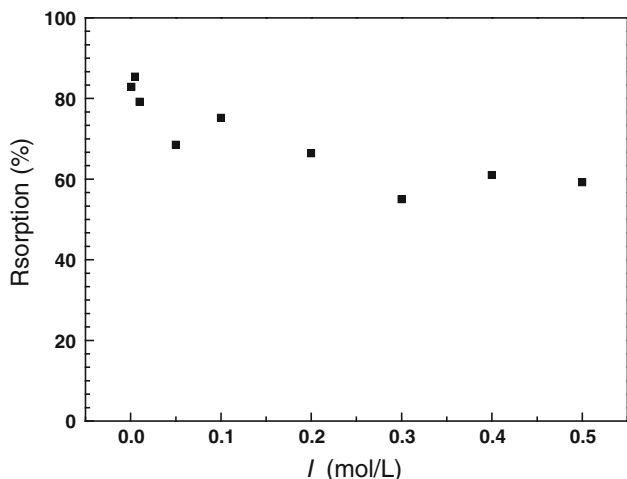


**Fig. 5** Effect of ionic strength on the sorption of Th(IV) on GO.  $T = 25 \pm 1 \text{ }^\circ\text{C}$ ,  $m/V = 0.5 \text{ g/L}$ , and  $\text{pH} 2.80 \pm 0.05$

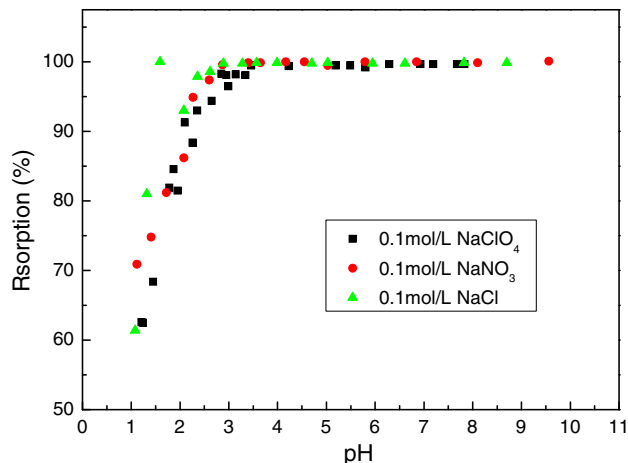


**Fig. 7** Effect of different anions on Th(IV) sorption on GO.  $T = 25 \pm 1 \text{ }^\circ\text{C}$ ,  $m/V = 0.5 \text{ g/L}$ , and  $\text{pH} 2.80 \pm 0.05$

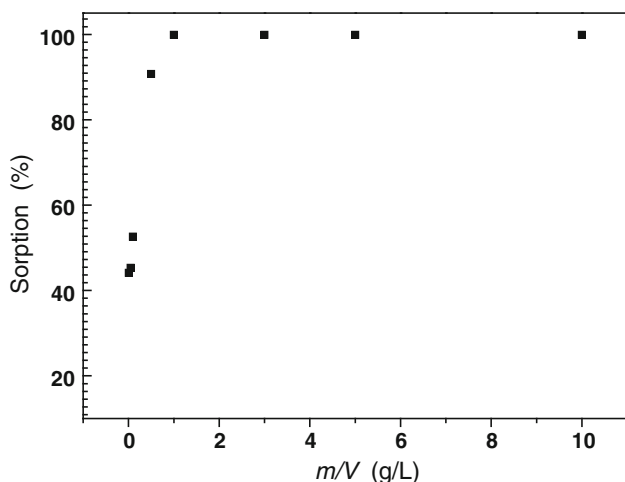


**Fig. 6** Sorption of Th(IV) on GO as a function of  $m/V$ .  $I = 0.1 \text{ mol/L NaCl}$ ,  $T = 25 \pm 1 \text{ }^\circ\text{C}$ , and  $\text{pH} 2.80 \pm 0.05$

increases with increasing mass of goethite, attapulgite, and  $\text{Zr}_2\text{O}(\text{PO}_4)_2$ . The sorption percentage of the metal ions also increased with increasing sorbent dose, which is only because of the greater surface area and the availability of more active sorption sites with increased sorbent dose.

Effect of foreign ions

The sorption of Th(IV) on GO was investigated with different background electrolyte solutions (Figs. 7, 8). The foreign anions drastically affect Th(IV) sorption on GO. From Fig. 7, the sorption of Th(IV) was lowest in 0.1 mol/L  $\text{NaClO}_4$  and highest in 0.1 mol/L  $\text{NaCl}$ , although the difference between the three electrolyte solutions was small. Figure 8 shows the sorption of Th(IV) on GO in 0.1 mol/L  $\text{LiCl}$ ,  $\text{NaCl}$ , and  $\text{KCl}$  solutions. The order of the

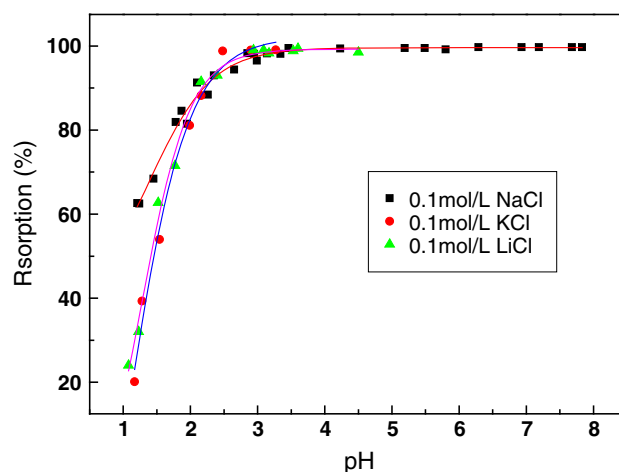


**Fig. 8** Effect of different cations on Th(IV) sorption on GO.  $T = 25 \pm 1 \text{ }^\circ\text{C}$ ,  $m/V = 0.5 \text{ g/L}$ , and  $\text{pH} 2.80 \pm 0.05$

hydrated radii of these monovalent cations is  $\text{Li}^+ > \text{Na}^+ > \text{K}^+$  ( $\text{K}^+$ : 2.32 Å,  $\text{Na}^+$ : 2.76 Å,  $\text{Li}^+$ : 3.4 Å [66]). Therefore, the hydrated  $\text{K}^+$  cation more easily interacts with the surface functional groups of the adsorbent than the hydrated  $\text{Na}^+$  and  $\text{Li}^+$  cations. A previous study concerning the sorption of Th(IV) on goethite [32] indicated that the distribution coefficient of the sorption of Th(IV) on goethite in  $\text{NaCl}$  solution was higher than that in  $\text{NaNO}_3$  solution at the same pH value.

Effect of humic and FA

Figure 9 shows the pH sorption edges of Th(IV) in the absence and presence of FA and HA. The sorption edge of Th(IV) in the presence of FA/HA is much lower than that in the absence of FA/HA. This result can be explained by

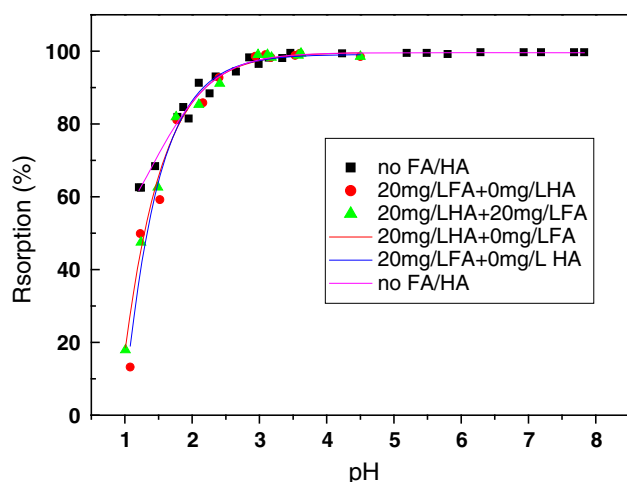


**Fig. 9** Sorption of Th(IV) to GO in the presence of FA and HA: pH  $2.80 \pm 0.05$ ,  $m/V = 0.5$  g/L, and  $I = 0.1$  M NaCl

the fact that in solution FA and HA form soluble complexes of Th–FA and Th–HA, and can stabilize Th(IV) in solution, thereby decreasing the sorption of Th(IV) on GO. On the other hand, there are also several changes in the morphology of GO in the presence of HA. For example, the interaction of the functional groups, the  $\pi$ – $\pi$  interaction between HA and GO, and the blocking of the interlayer by the large molecular size. Thus, HA can occupy the active sorption sites, which leads to a decrease in the sorption capacity. Under our experimental conditions, the formation of Th–FA and Th–HA complexes is the dominant factor in the effect of FA or HA. When HA was added to the system, there is competition between HA and Th(IV) for the GO surface sites, and hence there is a decrease in the sorption of Th(IV) on GO. Both HA and FA contain the same functional groups, although FA has more functional groups than HA. The very small difference between the influence of HA and FA in this work indicates that the functional groups of HA and FA almost equally contribute to the sorption under acidic conditions. The result is analogous to that of Th(IV) on Hematite [67].

## Conclusion

In conclusion, GO was synthesized from flake graphite by the modified Hummers method and characterized by a variety of methods. The sorption percentage of Th(IV) on GO decreased at high ionic strength and low solid-to-liquid ratio. The sorption edge of Th(IV) in the presence of FA/HA was much lower than that in the absence of FA/HA. The sorption processes of Th(IV) can be accurately described by a pseudo-second-order rate model. The maximum sorption capacity ( $C_{s,max}$ ) of Th(IV) at pH 2.8 and  $T = 298$  K was  $\sim 5.80 \times 10^{-4}$  mol/L. The rapid

sorption rate and large sorption capacity of GO suggests that the sorbent has very high adsorption efficiency and potential industrial applications. Thus, GO is a promising sorption material and has a high sorption capacity for Th(IV).

**Acknowledgments** We thank the National Natural Science Foundation of China (Grant Nos. 11075006 and 91026010), the Ministry of Education of the People's Republic of China (Grant No. 1002, 20120001110082), and the State Administration of Science Technology and Industry for National Defence (Grant Nos. 2007-840, 2012-851) for financial support.

## References

- Huang ZH, Zheng X, Lv W, Wang M, Yang QH, Kang F (2011) *Langmuir* 27(12):7558–7562
- Hirata M, Gotou T, Horiuchi S, Fujiwara M, Ohba M (2004) *Carbon* 42:2929–2937
- Park S, Ruoff RS (2009) *Nat Nanotechnol* 4:217–224
- Yang JT, Wu MJ, Chen F, Fei ZD, Zhong MQ (2011) *J Supercrit Fluid* 56:201–207
- Machida M, Yamazaki R, Aikawa M, Tatsumoto H (2005) *Sep Purif Technol* 46:88–94
- Kikuchi Y, Qian QR, Machida M, Tatsumoto H (2006) *Carbon* 44:195–202
- Shim JW, Park SJ, Ryu SK (2001) *Carbon* 39:1635–1642
- Strelko V, Malik DJ (2002) *J Colloid Interface Sci* 250:213–220
- Boehm HP (2002) *Carbon* 40:145–149
- Montes-Moran MA, Suarez D, Menendez JA, Fuente E (2004) *Carbon* 42:1219–1225
- Rivera-Utrilla J, Sanchez-Polo M (2003) *Water Res* 37:3335–3340
- Balog R, Jorgensen B, Wells J, Laegsgaard E, Hofmann P, Besenbacher F, Hornekaer L (2009) *J Am Chem Soc* 131:8744–8745
- Kim G, Jhi SH (2009) *J Phys Chem C* 113:20499–20503
- Leenaerts O, Partoens B, Peeters FM (2008) *Phys Rev B* 77(12):125416–125421
- Petit C, Bandosz TJ (2009) *J Phys Chem C* 113:3800–3809
- Romero HE, Joshi P, Gupta AK, Gutierrez HR, Cole MW, Tadigadapa SA, Eklund PC (2009) *Nanotechnology* 20:245501–245509
- Yang ST, Chang Y, Wang H, Liu G, Chen S, Wang Y, Liu Y, Cao A (2010) *J Colloid Interface Sci* 351:122–127
- Li ZJ, Chen F, Yuan LY, Liu YL, Zhao YL, Chai ZF, Shi WQ (2012) *Chem Eng J* 210:239–546
- Kütahyalı C, Eral M (2010) *J Nucl Mater* 396:251–256
- Metilda P, Gladis JM, Rao TP (2006) *Talanta* 68:1047–1064
- Qadeer R, Hanif J, Hanif I (1995) *J Radioanal Nucl Chem* 190:103–112
- Kaygun AK, Akyil S (2007) *J Hazard Mater* 147:357–362
- Fan QH, Wu WS, Song XP, Xu JZ, Hu J, Niu ZW (2008) *Radiation Environ Sci* 96:159–165
- Lu SS, Guo ZQ, Zhang CC, Zhang SW (2011) *J Radioanal Nucl Chem* 287:621–628
- Pan DQ, Fan QH, Li P, Liu SP, Wu WS (2011) *Chem Eng J* 172:898–905
- Sheng GD, Hu J, Wang XK (2008) *Appl Radiat Isot* 66:1313–1320
- Sharma P, Tomar R (2011) *J Colloid Interface Sci* 362:144–156
- Wu WS, Fan QH, Xu JZ, Niu ZW, Lu S (2007) *Appl Radiat Isot* 65:1108–1114



29. Guo ZJ, Niu LJ, Tao ZY (2005) *J Radioanal Nucl Chem* 266:333–338
30. Zhang HX, Zheng ZD (2006) *Tao Zy. Colloids Surf A* 278:46–52
31. Tan XL, Wang XK, Fang M, Chen CL (2007) *Colloids Surf A* 296:109–116
32. Yan L, Fan QH, Wu WS (2011) *J Radioanal Nucl Chem* 289:865–871
33. Chen CL, Wang XK (2007) *Appl Radiat Isot* 65:155–163
34. Östholms E (1995) *Geochim Cosmochim Acta* 59:1235–1249
35. Chen CL, Wang XK (2007) *Appl Geochem* 2:436–445
36. Chen CL, Li XL, Zhao DL, Tan XL, Wang XK (2007) *Colloids Surf A* 302:449–454
37. William S, Hummers J, Offeman R (1958) *J Am Chem Soc* 80:1339–1341
38. Li D, Kaner RB (2008) *Science* 320:1170–1171
39. Luo JY, Cote LJ, Tung VC, Tan ATL, Goins PE, Wu JS, Huang JX (2010) *J Am Chem Soc* 132:17667–17669
40. Anirudhan TS, Sreekumari SS, Jalajamony S (2013) *J Environ Radioact* 116:141–147
41. Guo ZJ, Li Y, Wu WS (2009) *Appl Radiat Isot* 67:996–1000
42. Zhang QH, Sun SY, Li SP, Jiang H, Yu JG (2007) *Chem Eng Sci* 62:4869–4874
43. Lu X, Yin QF, Xin Z, Zhang ZQ (2010) *Chem Eng Sci* 65:6471–6477
44. Noh JS, Schwarz JA (1990) *Carbon* 28:675–682
45. Yang ST, Chang YL, Wang HF, Liu GF, Chen S, Wang YW, Liu YF, Cao AN (2010) *J Colloid Interface Sci* 351:122–127
46. Deng XJ, Lu LL, Li HW, Luo F (2010) *J Hazard Mater* 183:923–930
47. Pimenta MA, Dresselhaus G, Dresselhaus MS, Cancado LG, Jorio A, Saito R (2007) *Phys Chem Chem Phys* 9:1276–1291
48. Paredes JI, Villar-Rodil S, Martinez-Alonso A, Tascon JMD (2008) *Langmuir* 24:10560–10564
49. Shen XP, Jiang L, Ji ZY, Wu JL, Zhou H, Zhu GX (2011) *J Colloid Interface Sci* 354:493–497
50. Al-Mashat L, Shin K, Kalantar-zadeh K, Plessis JD, Han SH, Kojima RW, Kaner RB, Li D, Gou X, Ippolito SJ (2010) *J Phys Chem C* 114:16168–16173
51. Zhao GX, Li JX, Ren XM, Chen CL, Wang XK (2011) *Environ Sci Technol* 45:10454–10462
52. Hosseini MS, Hosseini-Bandegharai A (2011) *J Hazard Mater* 190:755–765
53. Oke I, Olarinoye N, Adewusi S (2008) *Adsorption* 14:73–83
54. Deng XJ, Lu LL, Li HW, Luo F (2010) *J Hazard Mater* 183:923–930
55. Allen GC, Hubert S, Simoni E (1995) *J Chem Soc* 91:2767–2769
56. Krause M, Haire R, Keski-Rahkonen O, Peterson J (1988) *J Electron Spectrosc Relat Phenom* 47:215–226
57. Sharma P, Tomar R (2008) *Microporous Mesoporous Mater* 116:641–652
58. Bhattacharyya KG, Gupta SS (2006) *Adsorption* 12:185–204
59. Sharma A, Bhattacharyya KG (2005) *Adsorption* 10:327–338
60. Ngah WSW, Kamari A, Fatinathan S, Ng PW (2006) *Adsorption* 12:249–257
61. Monash P, Pugazhenth G (2009) *Adsorption* 15:390–405
62. Lützenkirchen J (1997) *J Colloid Interface Sci* 195:149–155
63. Goldberg S (2005) *J Colloid Interface Sci* 285:509–517
64. Yee N, Fein JB, Daughney CJ (2000) *Geochim Cosmochim Acta* 64:609–617
65. Qian LJ, Zhao JN, Hu PZ, Geng YX, Wu WS (2010) *J Radioanal Nucl Chem* 283:653–660
66. Zhang H, Yu XJ, Chen L, Geng JQ (2010) *J Radioanal Nucl Chem* 286:249–258
67. Reiller P, Casanova F, Moulin V (2005) *Environ Sci Technol* 39:1641–1648